Pure Appl. Chem., Vol. 85, No. 1, pp. 1–13, 2013.
http://dx.doi.org/10.1351/PAC-CON-12-04-10

Modeling complex biological systems: From solution chemistry to membranes and channels*

Benoist Laurent[1], Samuel Murail[1], Franck Da Silva[1], Pierre-Jean Corringer[2], and Marc Baaden[1,‡]

[1]Laboratoire de Biochimie Théorique, CNRS, UPR9080, Univ. Paris Diderot, Sorbonne Paris Cité, 13 rue Pierre et Marie Curie, 75005 Paris, France; [2]Institut Pasteur, Channel-Receptors G5 Group, CNRS URA 2182, Institut Pasteur, 25 rue du Dr Roux, 75015 Paris, France

Abstract: Complex biological systems are intimately linked to their environment, a very crowded and equally complex solution compartmentalized by fluid membranes. Modeling such systems remains challenging and requires a suitable representation of these solutions and their interfaces. Here, we focus on particle-based modeling at an atomistic level using molecular dynamics (MD) simulations. As an example, we discuss important steps in modeling the solution chemistry of an ion channel of the ligand-gated ion channel receptor family, a major target of many drugs including anesthetics and addiction treatments. The bacterial pentameric ligand-gated ion channel (pLGIC) called GLIC provides clues about the functional importance of solvation, in particular for mechanisms such as permeation and gating. We present some current challenges along with promising novel modeling approaches.

Keywords: cys-loop receptors; biomolecular chemistry; membranes; molecular dynamics; solution chemistry.

INTRODUCTION

Biological solutions are intrinsically complex and crowded mixtures. Some groups aim at modeling such systems in their full complexity, as illustrated by a snapshot of a recent simulation by McGuffee and Elcock endeavoring to understand diffusion properties of the bacterial cytoplasm (see Fig. 1A; [1]). However, such studies are currently limited to simplified approaches, such as Brownian dynamics of rigid molecules. Here, we investigate the more common case of studying a single protein in a realistic environment, using a fully flexible atomistic force field representation. For this purpose, we describe the example of a pentameric ligand-gated ion channel (pLGIC) called GLIC, illustrating how modeling may nowadays attempt to capture the complex "solutions" involved in biological processes.

pLGICs are membrane receptors widespread in the animal kingdom. The members of this family, the γ-aminobutyric acid receptor of type A ($GABA_AR$), glycine (GlyR), serotonin ($5\text{-}HT_3R$), and nicotinic acetylcholine receptors (nAChRs), play a leading role in the nervous signal transduction. Upon specific ligand binding (drawing the receptor name), an allosteric transition occurs leading to an open-

Pure Appl. Chem.* **85, 1–305 (2013). A collection of invited papers based on presentations at the 32nd International Conference on Solution Chemistry (ICSC-32), La Grande Motte, France, 28 August–2 September 2011.
‡Corresponding author

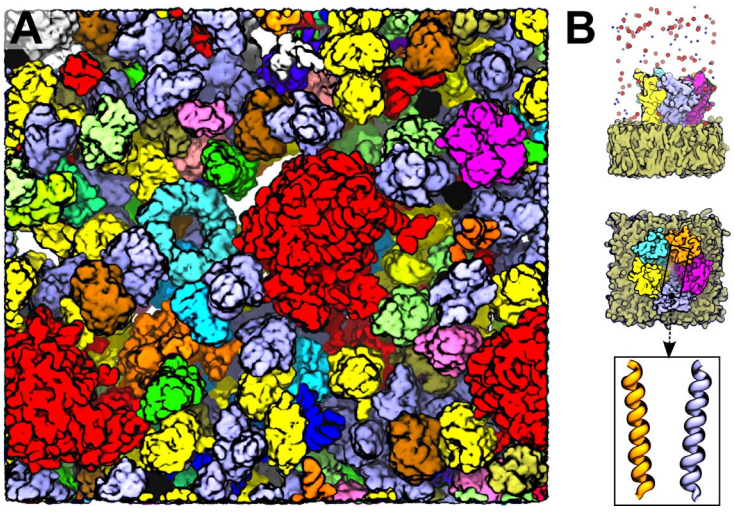

Fig. 1 (A) Snapshot of a bacterial cytoplasm model whose dynamics has been studied by Brownian dynamics (courtesy of Dr. Adrian Elcock [1]). (B) The GLIC system we study using MD simulations. The side view (top) displays the GLIC protein embedded in a phosphatidylcholine membrane in the presence of 150 mM NaCl. In the online version, the membrane is shown as an ochre surface, the protein is shown as yellow, cyan, orange, magenta, and blue surfaces, each color representing one of the five subunits. Sodium and chloride ions are displayed as blue and red spheres, while water is not shown for clarity. The top view (middle) depicts the five subunits, symmetrically arranged around the pore formed by the M2 helices (bottom panel showing two of the five helices lining the pore).

ing of the pore at the membrane level. This transition allows ions to enter the cell, producing a change in the electric potential across the membrane. The effect depends on the channel selectivity. In the case of cationic channels (nAChRs and 5-HT_3R), the entry of ions into the cell will lead to the depolarization of the cell and, if the membrane potential crosses a certain threshold (related to the number of open channels), the depolarization will propagate to initiate the action potential. On the other hand, the opening of anionic channels ($GABA_A$R and GlyR) will induce a hyperpolarization of the membrane potential and thus inhibits the action of cationic channels. Numerous compounds are known to modulate pLGIC function and channel activity, including some alcohols, steroids, cannabinoids, barbiturates, and general anesthetics. Membrane composition has also been shown to interfere with the activity of a few pLGICs. The example of nAChR is particularly striking, as cholesterol and anionic lipids are required for its activity [2].

Rational design of drugs acting on pLGICs recently came within reach owing to the crystallization of bacterial homologues, including the first open-channel structure of GLIC in 2009 [3,4]. While the role of the channel remains unclear for the bacteria, in vitro studies showed that GLIC is cation-selective and that its "gating", the process of opening and closing the channel, is regulated by pH variations [5]. The bacterial channel displayed several common characteristics with eukaryotic pLGICs, for instance, a very close 3-dimensional structure compared to a nematode glutamate-gated channel [6]. It also displayed sensitivity to alcohols and anesthetics [7,8].

pLGICs are transmembrane proteins constituted by five symmetrically organized subunits. The symmetry axis coincides with the central pore of the channel, where ion permeation takes place. The extracellular domain (ECD) of the protein contains the activating ligand-binding site and harbors a large vestibule for ions. The transmembrane domain (TMD) is structured in 4 helices per subunit called M1 to M4. The pore of the channel is lined by the M2 helices (Fig. 1B). Theoretical works suggest that the effective closure is due to a global twisting motion of the channel combined with local motions of the

transmembrane helices. In particular, the local motions comprise tilting associated with the bending of M2 [9–11].

Focusing on the case of GLIC, we discuss several challenges for the study of biological membrane protein solutions. Simplifications are necessary in constructing the model, in defining the composition of the system, and in choosing the concentration of each species. Uncertainties remain since neither experiments nor calculations can resolve issues such as reliably choosing the protonation states of each of GLIC's titratable groups. We discuss intrinsic properties of the models that remain unclear at this time such as the behavior of water in hydrophobic nanoconfinement.

THE COMPOSITION OF BIOLOGICAL "SOLUTIONS" IS COMPLEX

Biological solutions of interest contain several ingredients including proteins, nucleic acids, sugars, ions, water and other small molecules (alcohols, anesthetics, etc.). Depending on the goal a study aims to achieve, it might be necessary to include all these compounds in a model used for molecular dynamics (MD) simulations.

Cells communicate with each other thanks to membrane-embedded receptors whose hydrophobic TMDs are stabilized by the membrane environment. Hence, lipid bilayers or bilayer mimetics have to be included in a realistic model. Typical biological membranes are themselves complex ensembles composed of lipids, carbohydrates, proteins, and cholesterol in the case of eukaryotic cells [12]. The proportion of each molecular species depends on the cell type. Furthermore, different types of phospholipids are mixed in the membranes, with proportions again depending on the cell type and possible leaflet asymmetry. Matrix protein networks may further structure the membrane. To make the membrane picture more intricate, microdomains enriched in cholesterol, also called "lipid rafts", could play a role in the cellular function by compartmentalizing specific lipids and membrane proteins. However, the existence and role of such microdomains are very controversial.

Although some MD simulation studies now attempt to accurately model the complexity of, e.g., the *Escherichia coli* bacterial membranes [13], generally speaking such a complexity is very difficult to reproduce and the composition of the membrane is often simplified by using a single type of phospholipid. As an example, the GLIC simulation system is composed of the protein embedded in a fully hydrated phosphatidylcholine membrane, whereas a typical synaptic plasma membrane contains cholesterol (29 %), phosphatidylcholine (28 %), phosphatidylethanolamine (26 %), phosphatidylserine (10 %), phosphatidylinositol (2 %), sphingomyelin (2 %), and glycolipids (3 %) [14]. Unfortunately, our knowledge about lipid compositions of various organisms and cell types is still very limited, yet it is established that lipid "building blocks" have the potential to generate up to tens of thousands of different molecular species [15]. This situation may improve with recent efforts in the field of lipidomics [16].

When appropriate, ligands such as alcohols or general anesthetics are included in the model in order to study binding to the channel and modulation of its functional properties related to permeation and gating. The ligands may have indirect effects on the channel by interacting with the membrane and altering its behavior.

On the order of 150 mM NaCl or KCl ions are typically added to mimic physiologic electrolyte concentration. Sometimes higher concentrations up to 1 M are used to enhance the probability of processes such as ion permeation. These processes may be driven by cross-membrane potentials, which are typically in the range of –90 to –40 mV. To reproduce such a potential in the simulation may require special methods such as applying an electric field using additional forces on all charged particles [17]. Maintaining a charge imbalance between two solution compartments has initially been proposed by Sachs et al. [18]. This approach has subsequently been used by several groups to study the permeation of ion channels [19,20]. Herrera and Pantano proposed a variation of the method where ionic motion is restricted anisotropically to one side of the system [21]. Finally, Bostick et al. used vacuum slabs to separate the compartments of a single unit cell [22]. A set-up to study ion permeation through GLIC using

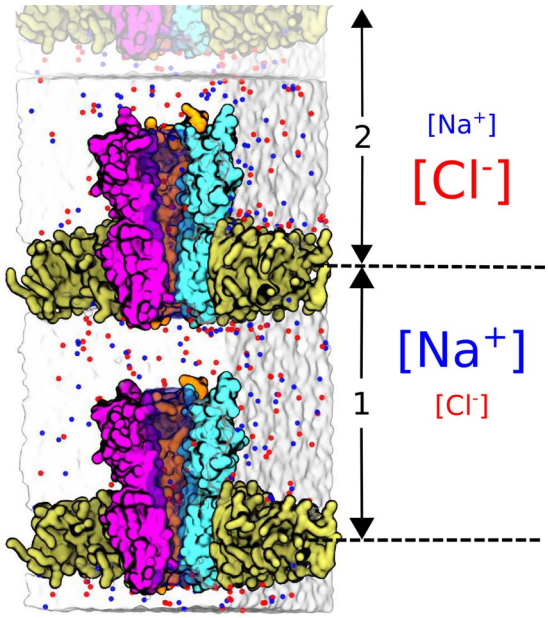

Fig. 2 System set-up used to study ion permeation through GLIC according to the double bilayer method [19]. The two compartments display different ion concentrations that create an electric potential between them, driving the ions through the channel. Only three of the five protein subunits and half of the membrane are represented in order to expose the pore interior, displayed as a blue transparent surface (in the online version).

the double bilayer approach is shown in Fig. 2. The intrinsic electrostatic field of GLIC guiding the ions through its center is illustrated in the following movie.

An animation of the electrostatic field around GLIC was generated using BioBlender (http://bioblender.eu/) followed by post-processing in our in-house UnityMol tool. A movie illustrates the flow of electric field lines through the ion channel. It is available at http://www.baaden.ibpc.fr/pub/glic/pac.mov.

CONCENTRATION

Defining molecular concentrations at the microscopic level is not straightforward. Most simulation studies aim to match experimental conditions. Yet, due to limited computational resources, simulation "boxes" are typically designed as small as possible, focusing on the immediate membrane environment of the channel of interest and minimizing the bulk solvent part. This introduces a bias in the calculation of concentrations.

In many experiments involving membrane proteins, a salt concentration of about 150 mM NaCl is required to warrant an appropriate osmotic pressure. The number of Na^+ and Cl^- ions to add to a simulation system may be calculated using eq. 1 with C_{water} = 55 M. The calculated number of ions is adjusted to neutralize the global charge of the system (i.e., protein charges), hence in this case $N_{Na} \neq N_{Cl}$. For the highly charged GLIC channel, there is an important imbalance between positive and negative ions, in our simulations typically about 90 Cl^- and 50 Na^+ are present. These numbers correspond to a concentration of about 150 mM when calculated on the basis of the Cl^- ions or 80 mM on the basis of the Na^+ ions. If the system was much larger (as in Fig. 3B), with an extensive bulk solvent part, this difference would progressively become negligible, tending toward $N_{Na} \sim N_{Cl}$.

$$N_{Na} = N_{Cl} = N_{water} \times C_{NaCl}/C_{water} \quad (1)$$

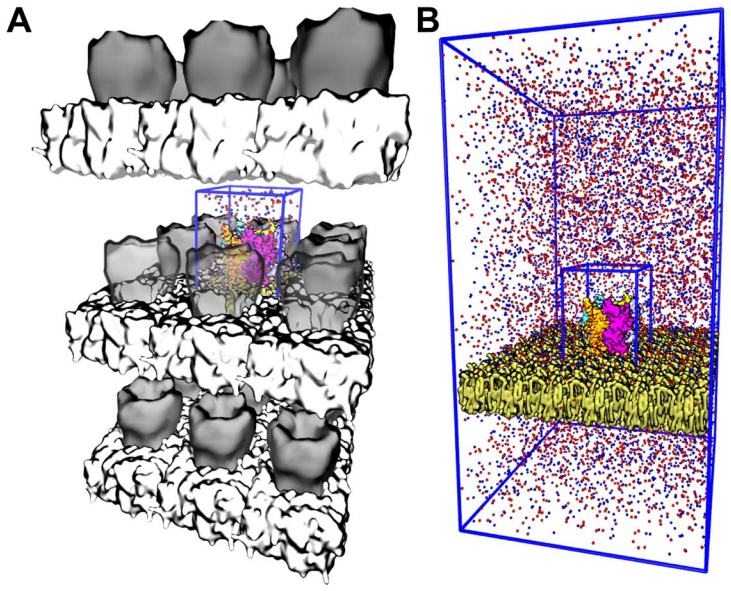

Fig. 3 (A) The 150 000 atoms atoms GLIC simulation system used for MD (colorized in the online version) surrounded by its periodic images. Since the simulation box is relatively tight, the replicates are very close to the original system, minimizing the bulk water and restricting membrane fluctuations. (B) An imaginary system in which the bulk water is extended and the membrane is large enough to allow for medium-range fluctuations, leading to a significant increase in the number of atoms beyond 4 000 000. For comparison, the periodic box of the 150 000 atoms system is also represented.

Ion concentration could in principle constitute a way to study the influence of pH by explicitly adding protons to the simulation system [23]. However, this approach is impractical in the present case because a huge simulation box would be required: at pH 4.6, a box containing 2 189 589 water molecules is necessary to observe a single H^+ ion, i.e., 50 times the actual simulation box size we use for GLIC. This echoes the fact that the number of water molecules in simulations is generally too low to mimic dilute solutions. A higher ratio of water to (protein + membrane) would be required to properly account for bulk concentrations.

Furthermore, concentration is a dynamic property. Brannigan et al. reported simulations in which they flooded both GLIC and nAChR receptors with isoflurane, a general anesthetic. During the simulation an important number of the hydrophobic isoflurane molecules partition into the lipid bilayer. Hence, at the end of the simulation, the concentration of isoflurane in the solvent is significantly lower (<10 mM) than when it started (>100 mM). This process is depicted on Fig. 4 along with data for alcohol partitioning [24].

Brannigan's study implies that a long equilibration of the system may be necessary before concentrations can be measured reliably in order to allow solute molecules to partition between aqueous and membrane phases. It may be debated whether concentrations should be calculated with respect to the water phase only, with respect to water and membrane or with respect to the entire simulation box.

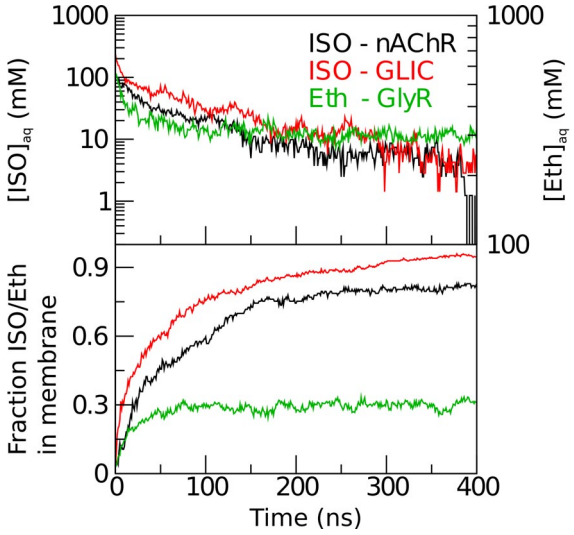

Fig. 4 Isoflurane (black and red in the online version) and ethanol (green in the online version) partition into the membrane during the equilibration of a GLIC, a nAChR and a GlyR system, respectively. The aqueous concentration of isoflurane (top) decreases for the benefit of the fraction in the membrane (bottom). The same behavior is observed for the partitioning of ethanol during the equilibration of a GlyR system (green in the online version) but to a lesser extent. Due to its more hydrophilic properties, ethanol concentration decreased to half the initial one (~300 mM) at the end of the simulation. This is in contrast to isoflurane: its concentration drops to less than 10 % of the starting one (~10 mM).

PROTONATION STATE

Knowing the protonation state of ionizable residues is a key issue to reliably model a protein. The protonation state depends on a residue's local environment. Standard pK_a values measured in bulk cannot be applied to buried protein residues, in particular for membrane proteins with an environment that largely differs from aqueous solution. GLIC is constituted of five symmetric protomers, and the location of its 81×5 ionizable residues is shown in Fig. 5. We may consider that equivalent residues in each subunit bear identical protonation states. This assumption leads to approximately $2^{81} = 10^{19}$ possible combinations of protonation states. Tang and co-workers suggest that the protonation state of some titratable groups may be different from one protomer to another leading to up to 10^{98} different combinations [25,26], a figure exceeding the number of particles in the universe!

The development of methods for calculating pK_a values of titratable groups in proteins was pioneered by Tanford and Kirkwood who proposed to represent the protein as an impenetrable sphere, which allows one to analytically solve the Poisson–Boltzmann equation (PBE) [27]. The increase in computing performances has facilitated the development of many PBE solvers, including the widely used APBS software [28,29]. Nielsen and co-workers showed that a finite difference Poisson–Boltzmann method yields better results when adding an explicit step to optimize the hydrogen-bond network [30]. Ideally, protein conformational flexibility should be taken into consideration for calculating pK_a values. Specific terms have been included in some algorithms [31] and, more recently, methods based on the λ-dynamics approach using constant pH MDs and replica exchange MD emerged [32–34]. These latter methods are currently still under development and have so far only been tested on small nonmembrane peptides or proteins. PROPKA [35,36] may be one of the most commonly used empirical approaches because it is very fast.

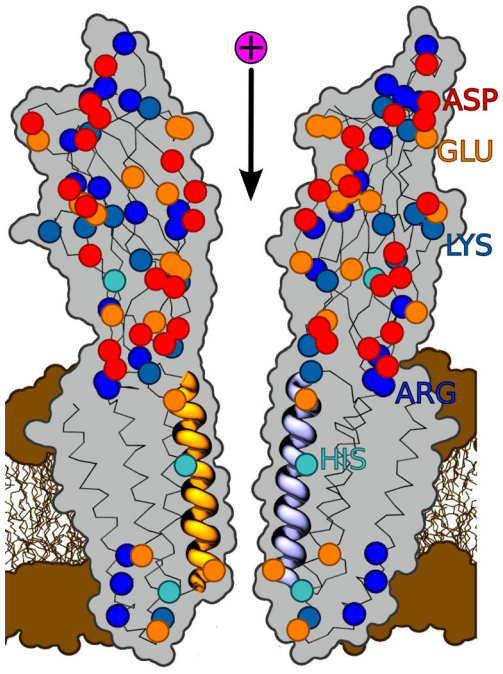

Fig. 5 Localization of ionizable residues shown in a cross-section of the GLIC ion channel (gray). M2 helices, in cartoon representation, line the pore through which cations (pink in the online version) cross the membrane (ochre in the online version).

In order to set up simulations of the GLIC system, we assessed the results of several widely used programs and web services. These pK_a predictions yielded widely varying pK_a shifts as illustrated in Fig. 6. We settled on the use of the Yasara software [37] mixing Ewald summation and hydrogen-bonding network optimization to determine if a titratable group should be protonated or not [38]. The Yasara results remain in a reasonable pK_a shift range, whereas some of the other methods suggest huge shifts (Fig. 6). We applied a consensus approach, only protonating residues that were simultaneously found to change ionization state in all five subunits. Many efforts in improving the crystallization protocol for GLIC recently lead to a higher-resolution structure in which ion binding can be predicted between residue D86 and D88. This is a strong indication that these residues should not be protonated (unpublished data). These findings allowed us to iteratively improve our protonation state estimate for GLIC.

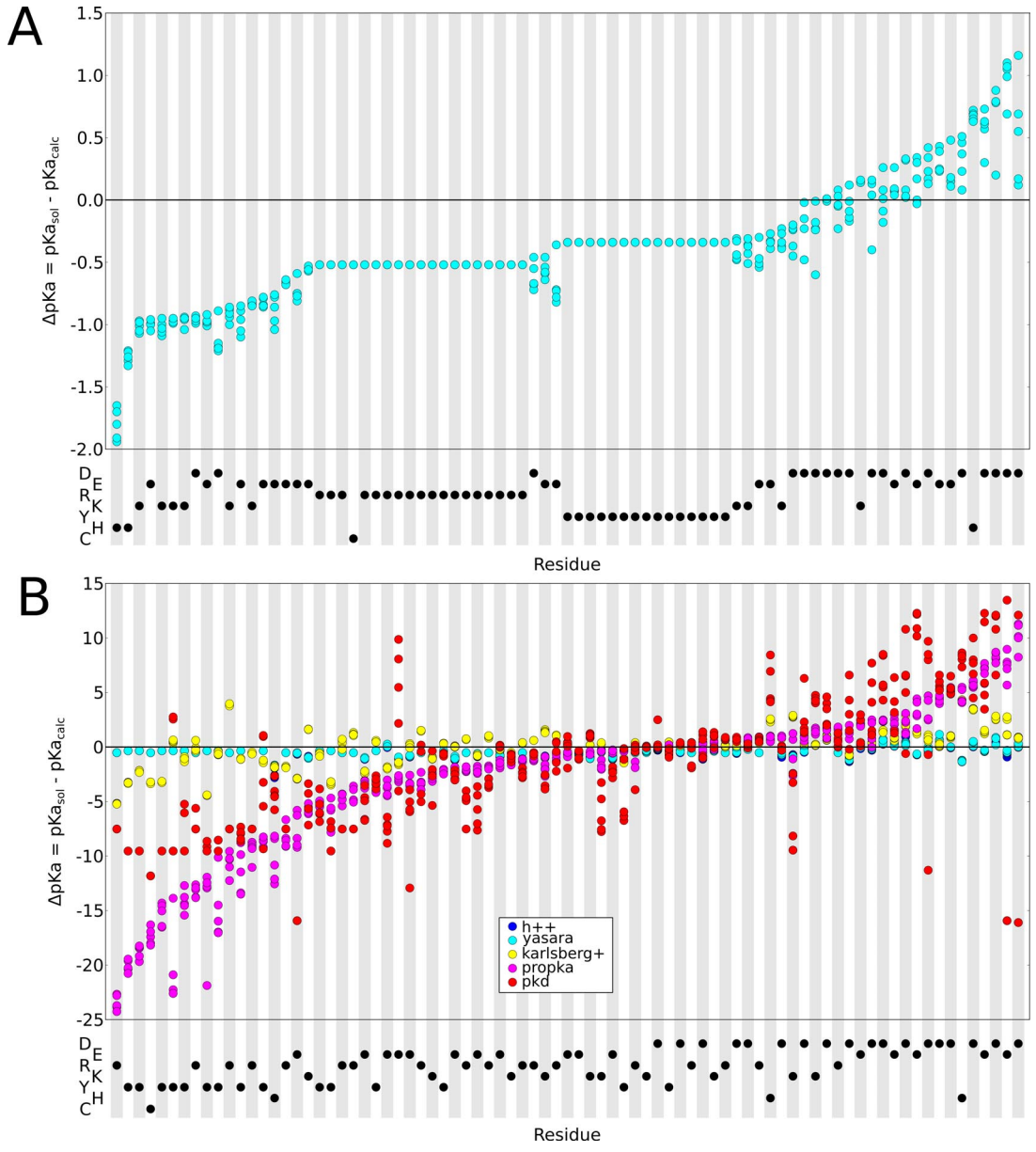

Fig. 6 pK_a shift predictions with respect to standard values for all ionizable residues in GLIC obtained using different software packages. Residues are ordered according to $\Delta pKa = (pKa_{solution} - pKa_{calc})$ with respect to the Yasara software (A) or the PROPKA software (B), respectively. The bottom part of each panel indicates the amino acid type of each residue.

SOLVATION IN SPECIAL/UNUSUAL ENVIRONMENTS

The complex shapes of proteins may feature channels and cavities providing special, potentially solvated nano-environments. Water in such a hydrophobic nanoconfinement may be particularly unstable, a phenomenon known as capillary evaporation. Several groups have observed and characterized dewetting transitions in MD simulations, for example, in the context of nanopores [39,40] or in the bacterial

mechanosensitive channels MscL and MscS [41,42]. Roth and co-workers suggest that capillary evaporation could constitute an intrinsic property of some channels [43] and may be a widespread biological mechanism.

In the case of GLIC, extensive sampling led us to observe an unexpected pore dewetting behavior (see Fig. 7A), as did several other groups [26,44]. Yet we cannot currently conclude whether GLIC belongs to a family of "bubble gated ion channels", since ongoing studies in our lab suggest that subtle changes in the simulation parameters may prevent dewetting from occurring (see Fig. 7B). Another very recent study is more affirmative [45]. It should be noted that forcefield parameters generally have not been tuned to reproduce the behavior of water in such special environments, which is in part due to the lack of experimental data.

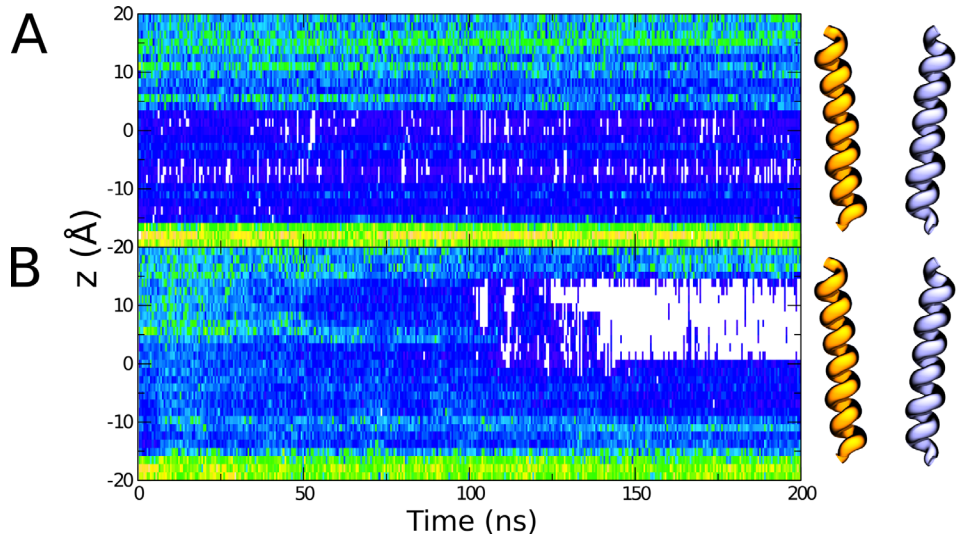

Fig. 7 Hydration traces of GLIC's pore during two representative simulations. Minor changes in the simulation parameters can make a noticeable difference between a fully hydrated channel (A) and a channel that dehydrates spontaneously in the upper part of the M2 helix-lined pore (B). For both simulations, the protonation states were identical [3], the only differences were the forcefield and the MD software used (amber99 and Gromacs for simulation A, vs. Charmm22 and NAMD2 for simulation B).

SAMPLING, STATISTICS, TIMESCALE

A fundamental question before starting any computational study is how to best spend the limited amount of available computing time. Strategies may vary in between two extremes: (1) running many short simulations from several starting points or (2) running an extended one-shot simulation. Shaw et al. recently showed that the result of the second approach matches experimental data very well, when the MD simulations are long enough [46].

In 2010, we studied GLIC gating in a 1 μs MD simulation suggesting a "domino" gating mechanism in which subunits sequentially switch from an open to a closed conformation [9]. Despite the large amount of computational resources (approx. 10 months of calculations on a supercomputer in 2009, i.e., tens of years on a recent desktop machine), only two protomers had fully undergone this transition to a closed state at the end of the simulation, suggesting that a much longer simulation was required to achieve a complete gating transition in all five protomers. Longer simulations are also needed to characterize processes such as ion permeation. Since GLIC has a low conductivity of 8 pS, one should observe an estimated passage of only 3 ions per microsecond at –65 mV. A computationally cheaper

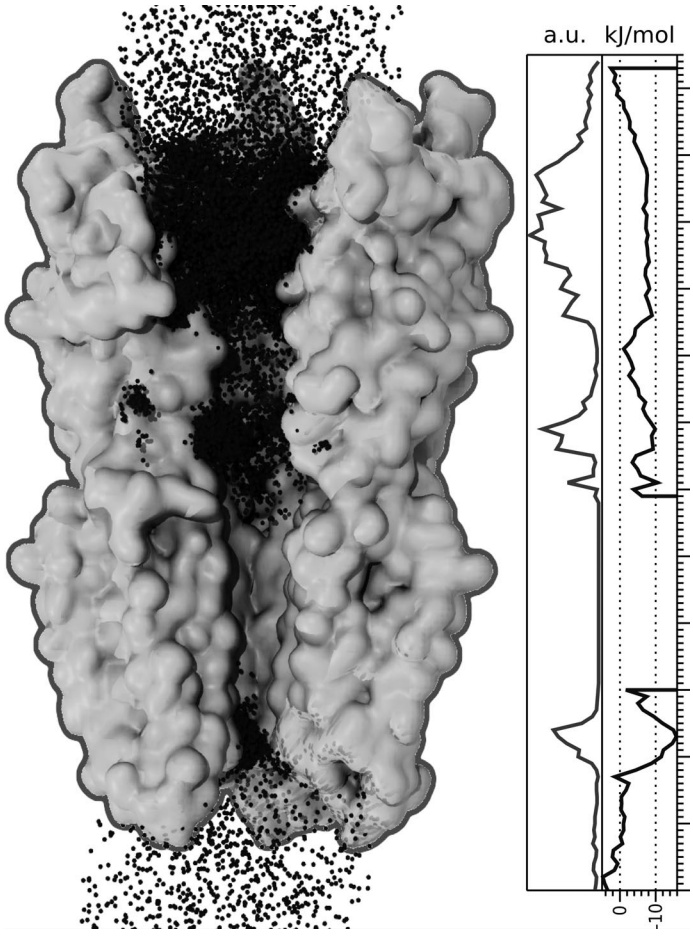

Fig. 8 Sodium ion occupancy and related relative Boltzmann energy accumulated during a 1-μs MD simulation.

alternative is to map the affinity of ions for a certain position along the channel pore. We have determined such a graph from the 1 μs gating simulation for a nonconductive state with a central barrier (Fig. 8). It is usually admitted that a simulation should be run at least 10 times longer than the slowest timescale of interest [47]. This is often impossible since many relevant biomolecular timescales exceed 1 μs. Typically, the neuromuscular acetylcholine receptor's gating is expected to be in the range of 1–10 μs [48] which implies MD simulations from 10 to 100 μs.

Running several short comparative simulations may be more appropriate for ligand binding studies, for example, involving drugs. An advantage of such short simulations is to remain close to a well-defined state, e.g., a crystal structure, rather than moving away from the experimentally backed conformation to some transient intermediate state. Furthermore, one may reduce the number of unproductive runs where the drug may diffuse out of the binding pocket into the solvent. Many short simulations with slightly different ligand starting conformations improve statistics and sampling. We employ such an approach to study two general anesthetics, propofol and desflurane, that have recently been co-crystallized with GLIC [49]. This study revealed a binding site in the upper part of the TMD of the protein. Other binding sites for general anesthetics and alcohols, including transmembrane, extracellular, and pore sites, have been suggested [8,25,50,51]. Channel blocking by charged quaternary ammonium compounds, divalent ions, and lidocaine has been shown using electrophysiology and X-ray

crystallography [52], also suggesting binding sites located in the pore of the channel. These observations pose the problem of sampling from a combinatorial point of view: multiplying the number of sites by the number of ligands, then by the number of mutants one wishes to test quickly leads to an intractable required total simulation time.

Lipids are crucial for the structure and function of membrane proteins. Bilayers with complex compositions pose a particular sampling challenge [53]. A misplaced lipid in a simulation set-up might have consequences on the whole trajectory, in particular if it were to play a specific biological role. With a diffusion coefficient of the order of 10^{-8} cm^2/s, a lipid embedded in a membrane is expected to have a mean-square displacement of 4 nm^2 for a 1-μs-long simulation. In our GLIC simulations, convergence for this value sets on beyond 100 ns and fully stabilizes at about 500 ns. Hence, the timescale of most current studies does not allow for an extensive reorganization of lipids around membrane proteins. Parton et al. recently addressed this problem while simulating a whole vesicle, demonstrating the importance of lipid diffusion for protein aggregation [54]. The authors, however, highlight that the coarse-grained models are highly simplified and inevitably approximate the nature of the protein–lipid and protein–protein interactions. De Meyer et al. previously suggested the role of cholesterol in protein clustering using dissipative particle dynamics Monte Carlo and a more simplified model [55].

At last, the problem of simulation convergence should be raised briefly. Methods for the quantification of sampling have been proposed for several decades, yet none has been widely adopted. In 2000, Berk Hess proposed a method based on principal component analysis [56] that has been used by other groups to evaluate the convergence of a set of MD simulations [57,58]. Faraldo-Gómez and coworkers focus on convergence of membrane protein simulations, and although the timescale is relatively short by today's standards, their main findings are likely still valid. Their work concludes that structured TMDs converge relatively fast, even on a 10 ns timescale, but more mobile parts are undersampled. Grossfield et al. calculated 26 independent 100 ns MD runs of rhodopsin and found similar results [58]. To date, despite new method proposals [59–61], sampling quality is often tentatively assessed based on several simple criteria. A single descriptor may be monitored along a simulation until it reaches a stable value. The root mean square deviation (RMSD), which is a descriptor for molecular deformation, is a common but controversial criterion. A variation consists in stopping a simulation after a descriptor reaches an experimental reference value and remains close to it for a certain time. Another approach is to use several independent MD simulations with different starting points. When these simulations converge to a similar state, sampling is considered sufficient.

CONCLUSION

Accurately simulating complex biological systems such as the GLIC ion channel in a realistic environment remains a puzzle with some missing pieces. Choosing the composition of the model requires a compromise between biological accuracy and technical constraints imposed by the limited size of simulation boxes. Even simple quantities such as concentrations are not easy to map from the macroscopic world to the microscopic representation. For some systems, protonation state assessment is a particularly tricky and largely unsolved problem. The behavior of water in special environments such as nanocavities and pores is another open issue. Underlying these specific points is the general question of sampling and timescale. Furthermore, the chosen GLIC example is a rather simple membrane system. Other more challenging ones may include double bilayers [62], entire vesicles [63,64], fully decorated virion particles [65–68], or huge bilayer patches, each adding a set of specific questions on its own.

ACKNOWLEDGMENTS

The authors would like to thank Jérôme Hénin and Grace Brannigan for providing the original data of Fig. 4. We also thank Marie Prévost for her expertness on experimental measurements, Tyler Reddy and Daniel Parton for their insight into recent lipidomics studies. We thank the French Agency for Research

for funding (Grant ANR-2010-BLAN-1534). Molecular simulations were performed using HPC computing resources from GENCI-IDRIS and GENCI-CINES (Grant 2011072292 to Marc Delarue). B.L. would like to thank his funding organisms: the Servier Labs and the "Ecole Doctorale Interdisciplinaire Européenne Frontières du vivant ED474" doctoral program Liliane Bettencourt.

REFERENCES

1. S. R. McGuffee, A. H. Elcock. *PLoS Comput. Biol.* **6**, e1000694 (2010).
2. A. W. Dalziel, E. S. Rollins, M. G. McNamee. *FEBS Lett.* **122**, 193 (1980).
3. N. Bocquet, H. Nury, M. Baaden, C. Le Poupon, J. P. Changeux, M. Delarue, P. J. Corringer. *Nature* **457**, 111 (2009).
4. R. J. Hilf, R. Dutzler. *Nature* **457**, 115 (2009).
5. N. Bocquet, L. Prado de Carvalho, J. Cartaud, J. Neyton, C. Le Poupon, A. Taly, T. Grutter, J. P. Changeux, P. J. Corringer. *Nature* **445**, 116 (2007).
6. R. E. Hibbs, E. Gouaux. *Nature* **474**, 54 (2011).
7. Y. Weng, L. Yang, P. J. Corringer, J. M. Sonner. *Anesth. Analg.* **110**, 59 (2010).
8. R. J. Howard, S. Murail, K. E. Ondricek, P. J. Corringer, E. Lindahl, J. R. Trudell, R. A. Harris. *Proc. Natl. Acad. Sci. USA* **108**, 12149 (2011).
9. H. Nury, F. Poitevin, C. Van Renterghem, J. P. Changeux, P. J. Corringer, M. Delarue, M. Baaden. *Proc. Natl. Acad. Sci. USA* **107**, 6275 (2010).
10. F. Zhu, G. Hummer. *Biophys. J.* **97**, 2456 (2009).
11. F. Zhu, G. Hummer. *Proc. Natl. Acad. Sci. USA* **107**, 19814 (2010).
12. G. van Meer, D. R. Voelker, G. W. Feigenson. *Nat. Rev. Mol. Cell Biol.* **9**, 112 (2008).
13. T. J. Piggot, D. A. Holdbrook, S. Khalid. *J. Phys. Chem. B* **115**, 13381 (2011).
14. W. G. Wood, M. Cornwell, L. S. Williamson. *J. Lipid Res.* **30**, 775 (1989).
15. A. Shevchenko, K. Simons. *Nat. Rev. Mol. Cell Biol.* **11**, 593 (2010).
16. H. Alex Brown. *Curr. Opin. Chem. Biol.* **16**, 221 (2012).
17. J. Gumbart, F. Khalili-Araghi, M. Sotomayor, B. Roux. *Biochim. Biophys. Acta* **1818**, 294 (2012).
18. J. N. Sachs, P. S. Crozier, T. B. Woolf. *J. Chem. Phys.* **121**, 10847 (2004).
19. C. Kutzner, H. Grubmuller, B. L. de Groot, U. Zachariae. *Biophys. J.* **101**, 809 (2011).
20. S. J. Lee, Y. Song, N. A. Baker. *Biophys. J.* **94**, 3565 (2008).
21. F. E. Herrera, S. Pantano. *J. Chem. Phys.* **130**, 195105 (2009).
22. D. Bostick, M. L. Berkowitz. *Biophys. J.* **85**, 97 (2003).
23. M. Baaden, M. Burgard, G. Wipff. *J. Phys. Chem. B* **105**, 11131 (2001).
24. S. Murail, B. Wallner, J. R. Trudell, E. Bertaccini, E. Lindahl. *Biophys. J.* **100**, 1642 (2011).
25. M. H. Cheng, R. D. Coalson, P. Tang. *J. Am. Chem. Soc.* **132**, 16442 (2010).
26. D. Willenbring, L. T. Liu, D. Mowrey, Y. Xu, P. Tang. *Biophys. J.* **101**, 1905 (2011).
27. C. Tanford, J. G. Kirkwood. *J. Am. Chem. Soc.* **79**, 5333 (1957).
28. F. Fogolari, A. Brigo, H. Molinari. *J. Mol. Recognit.* **15**, 377 (2002).
29. N. A. Baker, D. Sept, S. Joseph, M. J. Holst, J. A. McCammon. *Proc. Natl. Acad. Sci. USA* **98**, 10037 (2001).
30. J. E. Nielsen, K. V. Andersen, B. Honig, R. W. Hooft, G. Klebe, G. Vriend, R. C. Wade. *Protein Eng.* **12**, 657 (1999).
31. E. G. Alexov, M. R. Gunner. *Biophys. J.* **72**, 2075 (1997).
32. S. Donnini, F. Tegeler, G. Groenhof, H. Grubmuller. *J. Chem. Theory Comput.* **7**, 1962 (2011).
33. S. L. Williams, P. G. Blachly, J. A. McCammon. *Proteins* **79**, 3381 (2011).
34. Y. Meng, A. E. Roitberg. *J. Chem. Theory Comput.* **6**, 1401 (2010).
35. H. Li, A. D. Robertson, J. H. Jensen. *Proteins* **61**, 704 (2005).
36. D. C. Bas, D. M. Rogers, J. H. Jensen. *Proteins* **73**, 765 (2008).
37. E. Krieger, G. Koraimann, G. Vriend. *Proteins* **47**, 393 (2002).

38. E. Krieger, J. E. Nielsen, C. A. Spronk, G. Vriend. *J. Mol. Graphics Model.* **25**, 481 (2006).
39. O. Beckstein, P. C. Biggin, M. S. P. Sansom. *J. Phys. Chem. B* **105**, 12902 (2001).
40. O. Beckstein, M. S. Sansom. *Proc. Natl. Acad. Sci. USA* **100**, 7063 (2003).
41. A. Anishkin, S. Sukharev. *Biophys. J.* **86**, 2883 (2004).
42. A. Anishkin, B. Akitake, K. Kamaraju, C. S. Chiang, S. Sukharev. *J. Phys.: Condens. Matter* **22**, 454120 (2010).
43. R. Roth, D. Gillespie, W. Nonner, R. E. Eisenberg. *Biophys. J.* **94**, 4282 (2008).
44. D. N. Lebard, J. Henin, R. G. Eckenhoff, M. L. Klein, G. Brannigan. *PLoS Comput. Biol.* **8**, e1002532 (2012).
45. F. Zhu, G. Hummer. *Biophys. J.* **103**, 219 (2012).
46. D. E. Shaw, P. Maragakis, K. Lindorff-Larsen, S. Piana, R. O. Dror, M. P. Eastwood, J. A. Bank, J. M. Jumper, J. K. Salmon, Y. Shan, W. Wriggers. *Science* **330**, 341 (2010).
47. D. M. Zuckerman. *Annu. Rev. Biophys.* **40**, 41 (2011).
48. S. Chakrapani, A. Auerbach. *Proc. Natl. Acad. Sci. USA* **102**, 87 (2005).
49. H. Nury, C. Van Renterghem, Y. Weng, A. Tran, M. Baaden, V. Dufresne, J. P. Changeux, J. M. Sonner, M. Delarue, P. J. Corringer. *Nature* **469**, 428 (2011).
50. Q. Chen, M. H. Cheng, Y. Xu, P. Tang. *Biophys. J.* **99**, 1801 (2010).
51. G. Brannigan, D. N. LeBard, J. Henin, R. G. Eckenhoff, M. L. Klein. *Proc. Natl. Acad. Sci. USA* **107**, 14122 (2010).
52. R. J. Hilf, C. Bertozzi, I. Zimmermann, A. Reiter, D. Trauner, R. Dutzler. *Nat. Struct. Mol. Biol.* **17**, 1330 (2010).
53. T. A. Soares, T. P. Straatsma. *Mol. Simul.* **34**, 295 (2008).
54. D. L. Parton, J. W. Klingelhoefer, M. S. Sansom. *Biophys. J.* **101**, 691 (2011).
55. F. J. de Meyer, J. M. Rodgers, T. F. Willems, B. Smit. *Biophys. J.* **99**, 3629 (2010).
56. B. Hess. *Phys. Rev. E* **62**, 8438 (2000).
57. J. D. Faraldo-Gomez, L. R. Forrest, M. Baaden, P. J. Bond, C. Domene, G. Patargias, J. Cuthbertson, M. S. Sansom. *Proteins* **57**, 783 (2004).
58. A. Grossfield, S. E. Feller, M. C. Pitman. *Proteins* **67**, 31 (2007).
59. A. Grossfield, D. M. Zuckerman. *Annu. Rep. Comput. Chem.* **5**, 23 (2009).
60. X. Zhang, D. Bhatt, D. M. Zuckerman. *J. Chem. Theory Comput.* **6**, 3048 (2010).
61. F. Zhu, G. Hummer. *J. Comput. Chem.* **33**, 453 (2012).
62. L. Darré, A. Tek, M. Baaden, S. Pantano. *J. Chem. Theory Comput.* **8**, 3880 (2012).
63. P. M. Kasson, E. Lindahl, V. S. Pande. *PLoS Comput. Biol.* **6**, e1000829 (2010).
64. H. J. Risselada, H. Grubmuller. *Curr. Opin. Struct. Biol.* **22**, 187 (2012).
65. A. Arkhipov, W. H. Roos, G. J. Wuite, K. Schulten. *Biophys. J.* **97**, 2061 (2009).
66. P. L. Freddolino, A. S. Arkhipov, S. B. Larson, A. McPherson, K. Schulten. *Structure* **14**, 437 (2006).
67. E. R. May, C. L. Brooks III. *J. Phys. Chem. B* **116**, 8604 (2012).
68. W. H. Roos, I. Gertsman, E. R. May, C. L. Brooks III, J. E. Johnson, G. J. Wuite. *Proc. Natl. Acad. Sci. USA* **109**, 2342 (2012).

